NUMERICAL SIMULATION AND STRUCTURE IMPROVEMENT ON CYCLONE PURIFIER FOR FRESH AIR TREATING

Shuhui Xu1, Minglian Zhou2, and Fenghua Duan1

1Beijing Institute of Civil Engineering and Architecture，Beijing 100044, China
2Mechanical and Electronics Control Engineering School of Beijing Jiaotong University,
Beijing 100044, China

ABSTRACT

Cyclone purifier has been conventionally used for separating particles from exhaustion. This paper, however, tried to develop a cyclone purifier for fresh air treatment in ventilation. Simulations were carried out based on continuity equation, momentum equation, RNG k-epsilon turbulent flow equation and Discrete Phase Model; the discrete griddings were both structural and non-structural; the software used was FLUENT. The separation efficiencies, pressure drops and the flow patterns of air in the cyclone purifier were simulated. Simulations show that the optimal incline angle of the impeller vane is 30º, and the best vane number is 12 within 2 - 5 m/s of air velocity in the cyclone purifier. Separation efficiency for particles size 10 micron is over 85 %, and pressure drop is less than 3.5 kPa. The simulations of separation efficiencies and pressure drop were verified by experiments.

KEYWORDS

Cyclone purifier, Numerical simulation, Pressure drop, Separation efficiency

INTRODUCTION

As cyclone purifier has many advantages, such as low pressure drop, simple structure, no moving parts, high reliability etc., it is very suitable for the fresh air treatment for the air conditioner, especially for some places the outdoor air has been badly polluted. The main structure of a cyclone purifier is an impeller in a pipe. When air goes through the pipe, the impeller makes it rotating, and the centrifugal force moves the particles in the air to the internal wall of the pipe and seized, and the clean air goes out the pipe. A horizontal pipe cyclone purifier for fresh air treating was developed in our research, and this paper reports the CFD simulation part of the development.

PHYSICAL MODEL AND MATHEMATICAL MODEL

The outline of the cyclone purifier is as shown in Figure 1. Air enters the cyclone purifier from inlet 1, goes through the impeller 2 in the pipe 3, impeller 2 forces air rotating. The centrifugal force moves the particles in the air to the internal wall of the pipe 3, and the particles are seized and pushed to the contaminant container 5, while the clean air goes out the pipe through outlet 6. The key part of the cyclone purifier is impeller, and the structure of the impeller is as shown in Figure 2. The main structural parameters of the impeller are outside diameter of the impeller D, inside diameter D_m, number of the vanes m, incline angle of vane α, length of the central guide rod L.

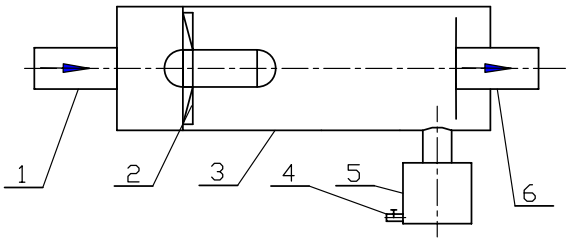

1-inlet, 2-impeller, 3-pipe, 4-valve,
5-contaminant container, 6-outlet
Figure 1 Outline of the cyclone purifier

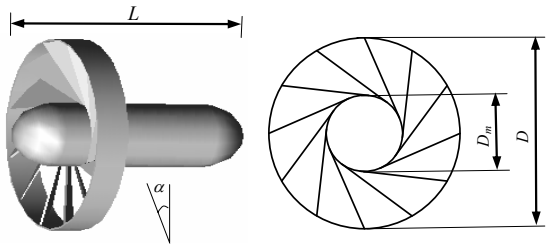

3-D view left view
Figure 2 Structure of the impeller

The physical model of the cyclone purifier was set up based on the actual size of the cyclone purifier. For calculation by FLUENT software with high convergence rate, the discrete griddings of both structural and non-structural were made, as shown in Figure 3 (Luo 2004).

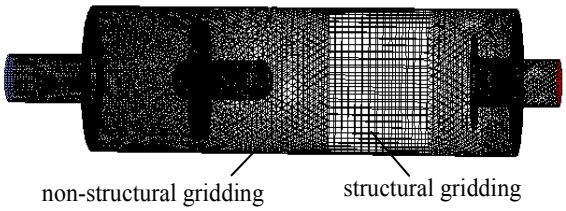

Figure 3 Gridding for numerical calculation

In a circular cylindrical coordinates (x, r, θ), the air velocities in different direction are respectively u, υ and w. As air velocity in the pipe is rather high, RNG k-ε model (Speziale and Thangam 1992, Smith and Reynolds 1992, Shih, et al. 1995, Lu 1999) was suitable for all flow in the pipe. The particles in the air were described by Discrete Phase Model from FLUENT 6.1, and SIMPLE method (Patankar S V. 1980, Tao WQ. 2001) was used in the calculation. Considered the symmetry of the geometry and flow, and ignored all differential terms of the tangent direction, the governing equations of the steady state fluid flow in the cyclone purifier were obtained as follow.

Continuity equation

$$\frac{\partial(\rho u)}{\partial x}+\frac{1}{r}\frac{\partial(r\rho\upsilon)}{\partial r}=0 \tag{1}$$

u-momentum conservation equation

$$\frac{\partial}{\partial x}(\rho uu)+\frac{1}{r}\frac{\partial}{\partial r}(r\rho\upsilon u)$$
$$=\frac{\partial}{\partial x}\left(\mu_e\frac{\partial u}{\partial x}\right)+\frac{1}{r}\frac{\partial}{\partial r}\left(r\mu_e\frac{\partial u}{\partial r}\right)+S_u \tag{2}$$

$$S_u=-\frac{\partial p}{\partial x}+\frac{\partial}{\partial x}\left(\mu_e\frac{\partial u}{\partial x}\right)+\frac{1}{r}\frac{\partial}{\partial r}\left(r\mu_e\frac{\partial \upsilon}{\partial x}\right) \tag{3}$$

υ-momentum conservation equation

$$\frac{\partial}{\partial x}(\rho u\upsilon)+\frac{1}{r}\frac{\partial}{\partial r}(r\rho\upsilon\upsilon)$$
$$=\frac{\partial}{\partial x}\left(\mu_e\frac{\partial \upsilon}{\partial x}\right)+\frac{1}{r}\frac{\partial}{\partial r}\left(r\mu_e\frac{\partial \upsilon}{\partial r}\right)+S_\upsilon \tag{4}$$

$$S_\upsilon=-\frac{\partial p}{\partial r}+\frac{\partial}{\partial x}\left(\mu_e\frac{\partial u}{\partial r}\right)$$
$$+\frac{1}{r}\frac{\partial}{\partial r}\left(r\mu_e\frac{\partial \upsilon}{\partial r}\right)-\frac{2\mu_e\upsilon}{r^2}+\frac{\rho w^2}{r} \tag{5}$$

w-momentum conservation equation

$$\frac{\partial}{\partial x}(\rho uw)+\frac{1}{r}\frac{\partial}{\partial r}(r\rho\upsilon w)$$
$$=\frac{\partial}{\partial x}\left(\mu_e\frac{\partial w}{\partial x}\right)+\frac{1}{r}\frac{\partial}{\partial r}\left(r\mu_e\frac{\partial w}{\partial r}\right)+S_w \tag{6}$$

$$S_w=-\frac{w}{r^2}\frac{\partial}{\partial r}(r\mu_e)-\frac{\rho\upsilon w}{r} \tag{7}$$

k equation

$$\frac{\partial}{\partial x}(\rho uk)+\frac{1}{r}\frac{\partial}{\partial r}(r\rho\upsilon k)$$
$$=\frac{\partial}{\partial x}\left(\frac{\mu_e}{\sigma_\varepsilon}\frac{\partial k}{\partial x}\right)+\frac{1}{r}\frac{\partial}{\partial r}\left(r\frac{\mu_e}{\sigma_\varepsilon}\frac{\partial k}{\partial r}\right)+S_k \tag{8}$$

$$S_k=G_k-\rho\varepsilon \tag{9}$$

ε Equation

$$\frac{\partial}{\partial x}(\rho u\varepsilon)+\frac{1}{r}\frac{\partial}{\partial r}(r\rho\upsilon\varepsilon)$$
$$=\frac{\partial}{\partial x}\left(\frac{\mu_e}{\sigma_\varepsilon}\frac{\partial \varepsilon}{\partial x}\right)+\frac{1}{r}\frac{\partial}{\partial r}\left(r\frac{\mu_e}{\sigma_\varepsilon}\frac{\partial \varepsilon}{\partial r}\right)+S_\varepsilon \tag{10}$$

$$S_\varepsilon=\frac{\varepsilon}{k}(C_1G_k-C_2\rho\varepsilon) \tag{11}$$

where

$$\mu_e=\mu+\mu_t$$

$$\mu_t=C_\mu\rho\frac{k^2}{\varepsilon}$$

$$G_k=\mu_t\left\{2\left[\left(\frac{\partial u}{\partial x}\right)^2+\left(\frac{\partial \upsilon}{\partial r}\right)^2+\left(\frac{\upsilon}{r}\right)^2\right]+\left(\frac{\partial u}{\partial r}+\frac{\partial \upsilon}{\partial x}\right)^2+\left[r\frac{\partial}{\partial r}\left(\frac{w}{r}\right)\right]^2+\left(\frac{\partial w}{\partial x}\right)^2\right\}$$

$$C_1=1.42-\frac{\eta(1-\eta/\eta_0)}{1-\beta\eta^3}$$

$$\eta=\frac{Sk}{\varepsilon}$$

$$S=\sqrt{2\bar{S}_{ij}\bar{S}_{ij}}$$

$C_\mu=0.085$, C_2=1.68, σ_k=0.7179

σ_ε=0.7179, β=0.015, $\eta_0=4.38$

NUMERICAL SIMULATION AND RESULT ANALYSIS

Impellers with following structure parameters were selected for the calculation: D=120 mm, D_m=40 mm. The pressure drop of the impeller, pressure drop of the cyclone purifier and the separation efficiency of the cyclone purifier were calculated respectively for L/D=1 and L/D=2; α=30º, α=45º and α=60º; m=8, m=10 and m=12, and their combinations. In the simulation, the velocity of the air in the cyclone purifier was defined as the average velocity in the purifier pipe where without impeller, and it ranged within 2 - 5 m/s.

Pressure drop simulation

When air flow through the cyclone purifier, impeller may cause pressure drop, and some partial eddies in the cyclone purifier may also create pressure drop. The pressure drop caused by the impeller with different m, α and L were simulated and processed in Figure 4, Figure 5 and Figure 6. The pressure drop of the whole cyclone purifier was also calculated and processed in Figure 7.

In Figure 4 ~ Figure 6, we can see that the pressure drop of the impeller increase as the increase of the air velocity constantly. When the impeller has more vanes, makes the area of the flow smaller, so the pressure

drop increased slightly. Smaller incline angle α, which changes the flow direction quicker, creates more pressure drop. A longer central guide rod, which diminishes the eddy flow to some extent, can hence decrease the pressure drop. However, the impeller pressure drop is no more than 240 Pa in all simulation, much less than the pressure drop of the cyclone purifier, compared Figure 4 ~ Figure 6 with In Figure 7. Hence to improve the structure of the cyclone purifier can decrease the pressure drop.

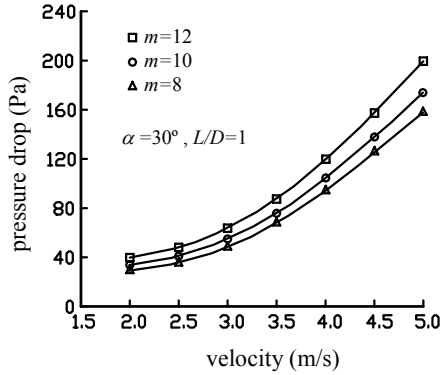

Figure 4 Impeller pressure drop, different m

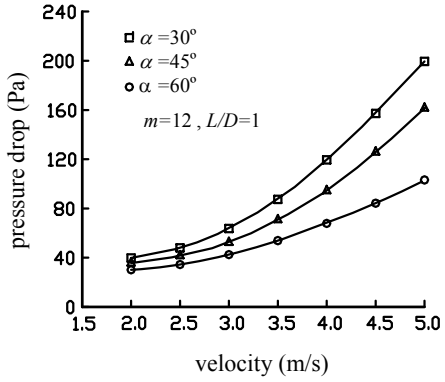

Figure 5 Impeller pressure drop, different α

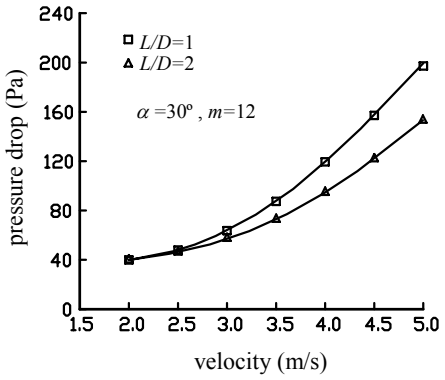

Figure 6 Impeller pressure drop, different L

Separation efficiency

The requirement of a cyclone is its low pressure drop and high separation efficiency. The simulation was carry out to calculate the separation efficiency of a cyclone purifier with different impellers of different α, different m, and L/D=1. The contaminant to be separated was water mist of 5 μm, 10 μm, 20 μm, 30μm respectively mixed in air. The results were shown in Figure 8 ~ Figure 11.

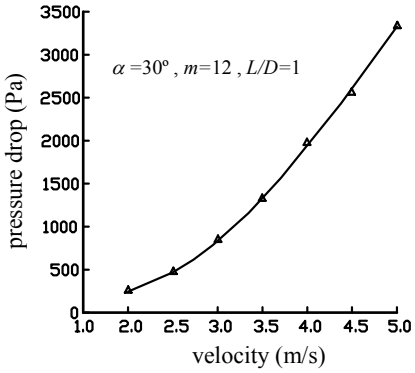

Figure 7 Pressure drop of the cyclone purifier

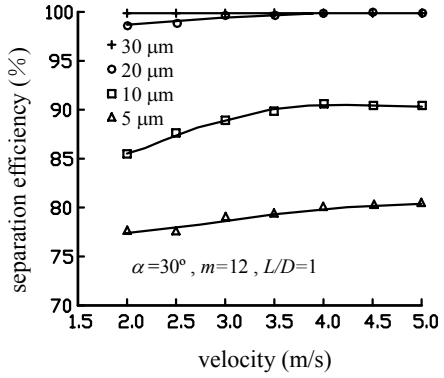

Figure 8 Separation efficiency, different size

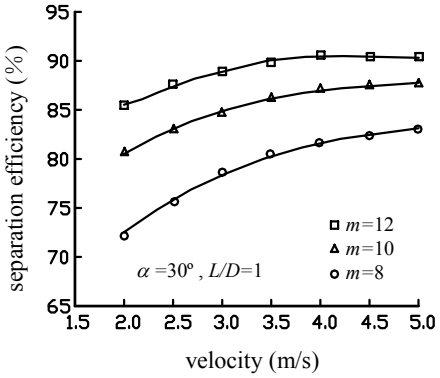

Figure 9 Separation efficiency, 10 μm, different m

In Figure 8, we find that the separation efficiency is increasing while the particles size increasing, and when the particle size is near 30 μm, nearly all particles are captured by the cyclone purifier. When the particles size is 10 μm, the separation efficiency is about 90%. When the particles size is smaller than 5 μm, the separation efficiency is less than 80%, so this type of cyclone purifier is not suitable for the fine dust separation.

Figure 9~Figure 11 compared the separation efficiency of 10 μm particles of the cyclone purifier with different impeller vane number m, different impeller incline angle α and different length of central guide rod L. The separation efficiency increases as the air velocity in the cyclone purifier increases. When the impeller has more vanes, it makes the flow more uniformly, and increases the separation efficiency. When the vane has a smaller incline angle α, it creates the flow rotation intensively, and increases the separation efficiency significantly, especially when the air flow velocity in the cyclone is low. And a longer central guide rod, in Figure 11, improves the flow in the cyclone, also increases the separation efficiency slightly.

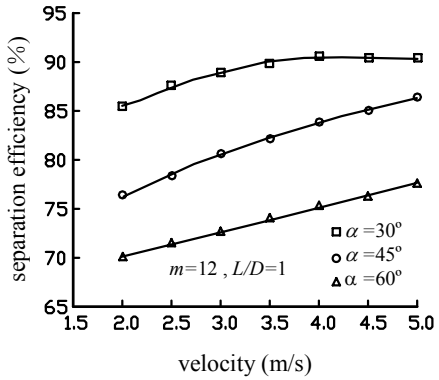

Figure 10 Separation efficiency, 10 μm, different α

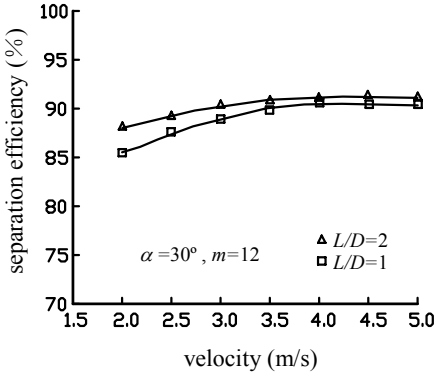

Figure 11 Separation efficiency, 10 μm, different L/D

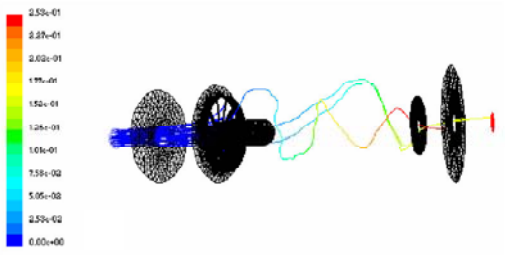

Figure 12 Trajectory visualization of 20 μm particles in the cyclone purifier

Particles separation visualization

For further investigating the separation process in the cyclone purifier, particles separation visualizations were simulated. Figure 12 ~ Figure 14 showed the trajectory of different size particles moving in the cyclone purifier when air velocity is 3 m/s. When the particles size is larger than 20 μm, most particles were captured, as shown in Figure 12; but when the size of particles is smaller than 5 μm, some particles escape from the cyclone purifier, as shown in Figure 14

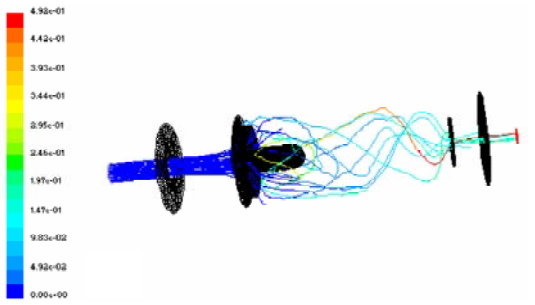

Figure 13 Trajectory visualization of 10 μm particles in the cyclone purifier

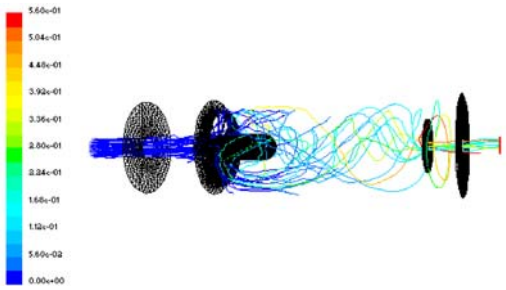

Figure 14 Trajectory visualization of 5 μm particles in the cyclone purifier

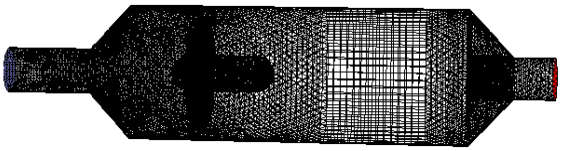

Figure 15 Gridding of improved cyclone purifier

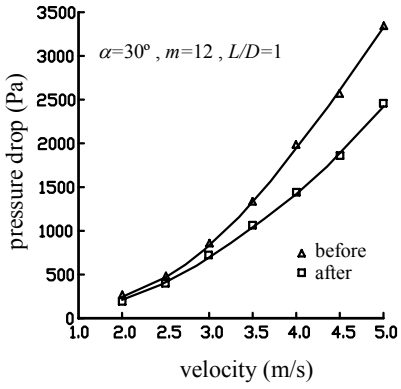

Figure 16 Pressure drop comparison,

before and after improved

SIMULATION OF THE IMPROVED CYCLONE PURIFIER

As mentioned in the previous section, the pressure drop caused by impeller is much smaller than the whole cyclone purifier. We tried to improve the shell structure of the cyclone purifier. Taper form of the pipe in both sides of the shell to eliminates the partial eddy, as shown in Figure 15. The pressure drop and separation efficiency of the improved cyclone purifier were simulated as shown in Figure 16 and Figure 17.

The improved cyclone purifier decreases pressure drop, especially when the air velocity is high. Meanwhile, the separation efficiency also improved slightly.

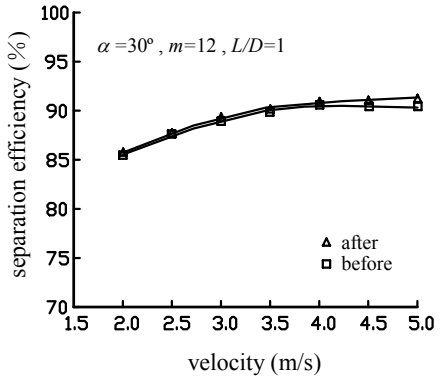

Figure 17 Separation efficiency comparison, 10 μm, before and after improved

EXPERIMENTAL STUDY

For the measurement of the specifications of the cyclone purifier and validation the simulation results, a cyclone purifier with the same structure as the simulated cyclone purifier was manufactured, its structure parameters were D=120 mm, D_m=40 mm, L/D=2, α=30º and m=12. A test system was set up as shown in Figure 18. In the experiments, the media was compressed air mixed with salt water of a certain concentration. The salt water was pumped by a water pump 13, and pulverized by a small air compressor 11 and a special nozzle 8. The size of water particles pulverized into the air was no more than 30 μm. The main stream compressed air was supplied by another air compressor 1.

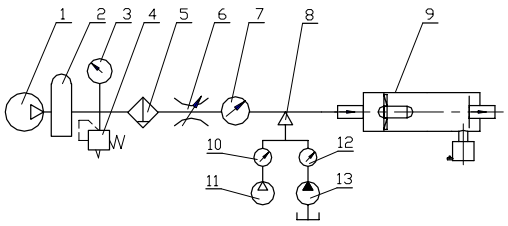

1-air compressor, 2-tank, 3-pressure meter, 4-relief valve, 5-separator, 6-regulator, 7-flow meter, 8-nozzle, 9-cyclone purifier, 10-air flow meter, 11-air compressor, 12-water flow meter, 13-water pump

Figure 18 Cyclone purifier test system

In the experiments, the pressure drop was measured with U tubes, and the results were compared with that of the calculation in Figure 19 and Figure 20.

The comparison shows that the simulation results fits the experiment result well, within the air velocity of 2 - 5 m/s, the average error of the impeller pressure drop is 3.2%, and the average error of the cyclone purifier pressure drop is 2.3%.

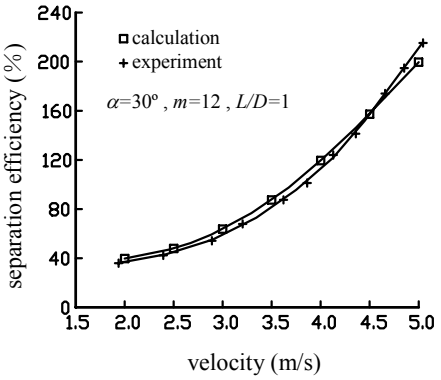

Figure 19 Impeller pressure drop comparison, calculation and experiment

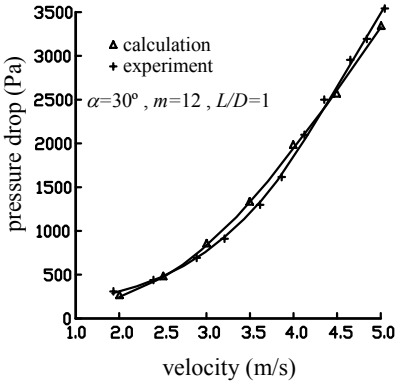

Figure 20 Cyclone purifier pressure drop comparison, calculation and experiment

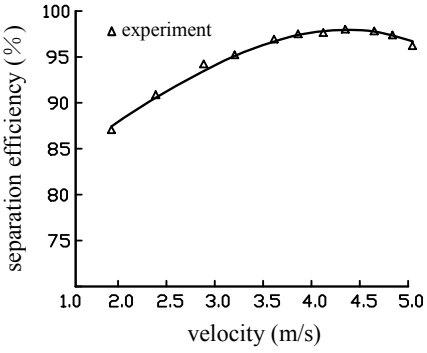

Figure 21 Separation efficiency of cyclone purifier

The test of the separation efficiency was a little complicated. In the experiments, the mass and

concentration of the salt water added into the air and the mass and concentration of the salt water captured by the purifier in the contaminant container was carefully measured in each working condition. During the separation process, it is inevitable that some water would be vaporized. Counting the change of concentration of the salt water to estimate and compensate the evaporation, the separation efficiency of the cyclone purifier was defined as

$$\eta_s = \frac{m_2}{m_1} \cdot \frac{y_2}{y_1} \times 100\% \quad (12)$$

where

η_s- the separation efficiency of the cyclone purifier

m_1 - the mass of the salt water added, kg

m_2 - the mass of the salt water captured by purifier, kg

y_1 - the concentration of the salt water added, kg/m^3

y_2 - the concentration of the salt water collected, kg/m^3

The separation efficiency of the cyclone changes with the increase of the air velocity, and the maximal efficiency of the cyclone purifier is 97.8%, and the maximal separation efficiency at the air velocity 4.3 m/s. When the air velocity is low, the rotation of the air is slow and centrifugal force can not separate some small particles. On the other hand, when the air velocity is too high, the turbulent flow carries some particles captured out of the purifier.

CONCLUSIONS

The simulations on the pressure drop, separation efficiency and particles separation visualization of cyclone purifier have been performed.

Numerical calculation results show that the pressure drop of the cyclone purifier is mainly created by air flow in the pipe, and impeller produced only very little pressure drop. Improvement on the structure of the pipe reduces the cyclone purifier's pressure drop significantly.

The simulations show that the optimal incline angle of the impeller vane is 30°, and best vane number is 12. The separation efficiency for particles size 10 μm is over 85%, and the separation efficiency for particles size 30 μm is nearly 100%.

Based on the simulation study above, a cyclone purifier was developed and tested. The maximum separation efficiency of the cyclone purifier is 97.8% for water particles no more than 30 μm, and the pressure drop is no more than 3 kPa.

ACKNOWLEDGMENT

Financial support from the Beijing College Academic Innovation Group Fund is gratefully acknowledged.

REFERENCES

Luo WB. 2004. "Numerical analysis and experimental study of vertical tube impeller cyclone purifier," Master degree Thesis, Beijing Institute of Civil Engineering and Architecture, 87 pages.

Speziale CG. and Thangam S. 1992. "Analysis of an RNG Based Turbulence Model for Separated Flows." International Journal Engineering Science, 30(2): 1379-1388.

Smith LM. and Reynolds WC. 1992. "On the Yakhot-orszag Renormalization Group Method for Deriving Turbulence Statics and Models." Physics of Fluid A, 4(4): 364-390

Shih TH, Liou WW, Shabbir A, etc. 1995. "A new *k-ε* eddy viscosity model for high Reynolds number turbulent flows". Computers Fluids,.24(3): 227-238.

Lu YH, Zhou LX, Shen X. 1999. "Numerical Simulation of Strongly Swirlling Turbulent Flows in Liquid-liquid Hydrocyclones Using RNG k-ε Model." Journal of hydrodynamics. 14(3): 325-333

Patankar SV. 1980. Numerical heat transfer and fluid flow. New York: Mc-Graw-Hill.

Tao WQ. 2001. Numerical Heat Transfer (Second Edition). Xian: Xian Jiaotong University Press